AD

AD-E403 035

Contractor Report ARAET-CR-04002

RIFILING PROFILE PUSH TESTS: AN ASSESSMENT OF BULLET ENGRAVING FORCES IN VARIOUS RIFLING DESIGNS

Jeff Siewert
Arrow Tech Associates
1233 Shelburne Rd., Suite D-8
S. Burlington, VT 05403

S. Cytron
ARDEC
Project Engineer

February 2005

ARMAMENT RESEARCH, DEVELOPMENT AND ENGINEERING CENTER

Armaments Engineering and Technology Center

Picatinny, New Jersey

REPORT DOCUMENTATION PAGE			*Form Approved* *OMB No. 0704-01-0188*

1. REPORT DATE (DD-MM-YYYY)	2. REPORT TYPE	3. DATES COVERED (*From – To)*
February 2005	Final	

4. TITLE AND SUBTITLE	5a. CONTRACT NUMBER DAAE30-00-M-0236
RIFLING PROFILE PUSH TESTS: AN ASSESSMENT OF BULLET ENGRAVING FORCES IN VARIOUS RIFLING DESIGNS	5b. GRANT NUMBER
	5c. PROGRAM ELEMENT NUMBER
6. AUTHORS	5d. PROJECT NUMBER
Jeff Siewert, Arrow Tech Associates S. Cytron, ARDEC, Project Engineer	5e. TASK NUMBER
	5f. WORK UNIT NUMBER

7. PERFORMING ORGANIZATION NAME(S) AND ADDRESS(ES)		8. PERFORMING ORGANIZATION REPORT NUMBER
Arrow Tech Associates 1233 Shelburne Rd. Suite D-8 S. Burlington, VT 05403	ARDEC, AETC Energetics, Warheads & Environmental Technology (AMSRD-AAR-AEE-P) Picatinny, NJ 07806-5000	
9. SPONSORING/MONITORING AGENCY NAME(S) AND ADDRESS(ES)		10. SPONSOR/MONITOR'S ACRONYM(S)
ARDEC, EM Technical Research Center (AMSRD-AAR-EMK) Picatinny, NJ 07806-5000		11. SPONSOR/MONITOR'S REPORT NUMBER(S) Contractor Report ARAET-CR-04002

12. DISTRIBUTION/AVAILABILITY STATEMENT

Approved for public release; distribution is unlimited.

13. SUPPLEMENTARY NOTES

14. ABSTRACT

This is the first in a series of reports aimed at assessing the influence of small caliber rifling designs on bullet engraving forces. The intent of this program is to evaluate the interior ballistics in gun barrels of unique rifling designs (e.g., polygonal) and/or bore materials (e.g., ceramic). This first report tests the assumption that engraving forces are related to the relative bore area of a small caliber gun barrel.

15. SUBJECT TERMS

Interior ballistics Rifling design Engraving force Polygonal rifling Small caliber

16. SECURITY CLASSIFICATION OF:			17. LIMITATION OF ABSTRACT	18. NUMBER OF PAGES	19a. NAME OF RESPONSIBE PERSON S. Cytron
a. REPORT U	b. ABSTRACT U	c. THIS PAGE U	SAR	40	19b. TELEPHONE NUMBER (Include area code) (973) 724-3368

Standard Form 298 (Rev. 8/98)
Prescribed by ANSI Std. Z39.18

CONTENTS

FIGURES

FIGURES
(continued)

FIGURES
(continued)

INTRODUCTION

The resistance force experienced by a small caliber projectile as it transitions from the cartridge case to the barrel forcing cone can significantly influence the interior ballistic performance of a given fixed cartridge. As part of the first report on this contract, it was assumed the engraving force was related to the relative bore area for a 7.62-mm gun barrel with varying rifling profiles. This assumption was tested and proved to be false, resulting in a change in recommended rifling profile.

OBJECTIVE

The objective of this study was to assess the effect of various gun and projectile parameters on engraving force (resistance pressure). The gun parameters examined were:

- Rifling profile (standard versus polygonal)
- Barrel forcing cone angle (1.2 deg versus 2.5 deg half angle)

The projectile parameters assessed were:

- External Lubrication (with and without spray-on solid film lube)
- Projectile configuration (composite versus solid)

METHOD

A production M240 gun barrel assembly was received from the sponsor for use as a control. The barrel (PN 11825987) was taken to a local National Guard armory for disassembly and removal of press-fit components. The configuration of the baseline M240 barrel is shown in figures 1 and 2.

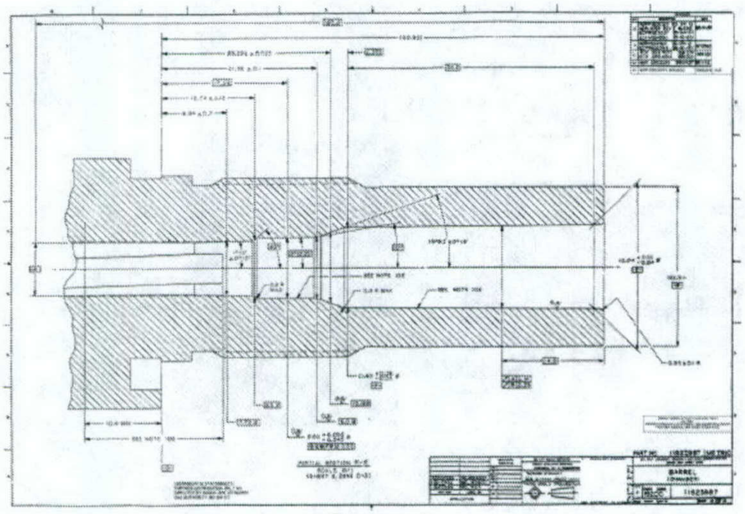

Figure 1
M240 chamber drawing

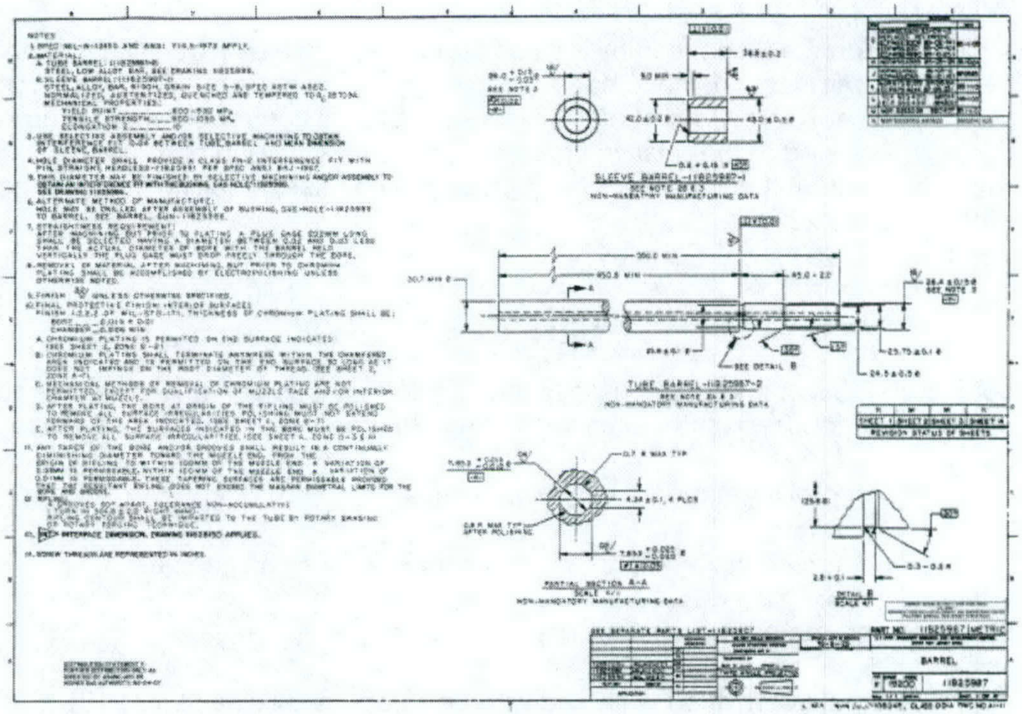

Figure 2
M240 barrel drawing

With the extraneous components removed, the bare barrel was taken to a local machine shop for modification. Figure 3 shows the machining sketch used by the machine shop to create the 2.5 in. long section used in the push test as a control.

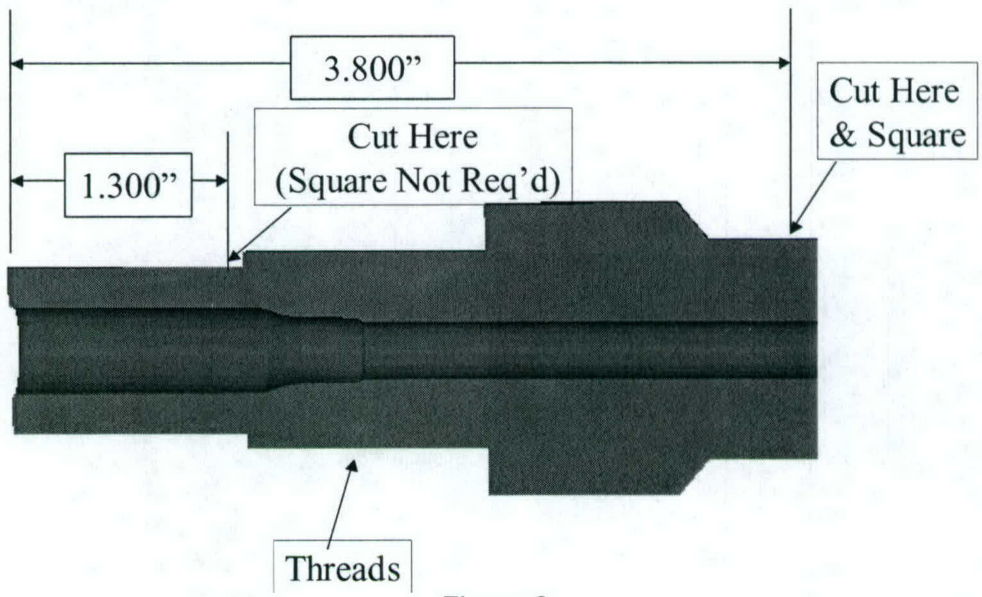

Figure 3
M240 baseline barrel (barrel 1) machining sketch

The second barrel section evaluated was a modification of the M240 baseline, it had a generic rifling configuration with a 2.5 deg half angle forcing cone versus the 1.2 deg half angle forcing cone found on the baseline barrel.

The modified barrel machining sketch (minus the forcing cone details) is shown in figure 4. The reamer for the modified forcing cone is shown in figure 5, while the dimensions for the reamer are listed in table 1.

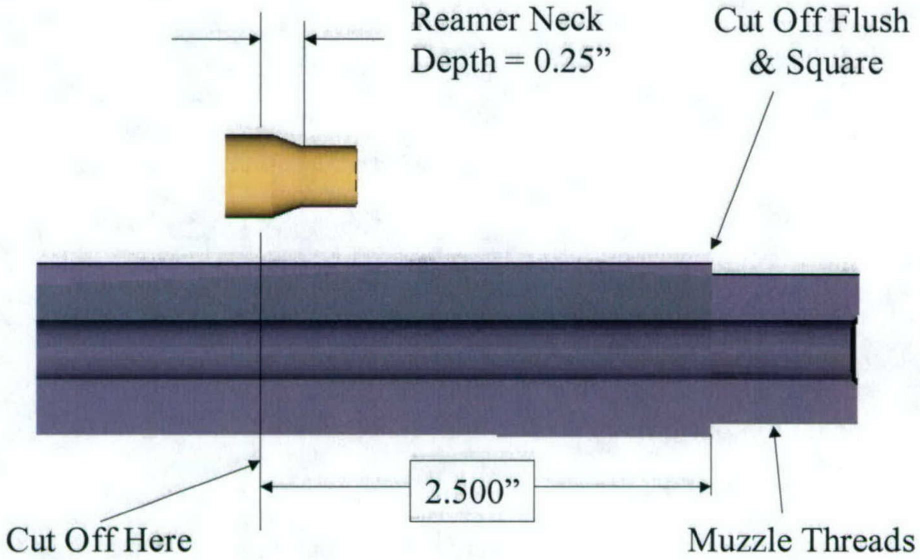

Figure 4
Modified M240 barrel (barrel 2) machining sketch

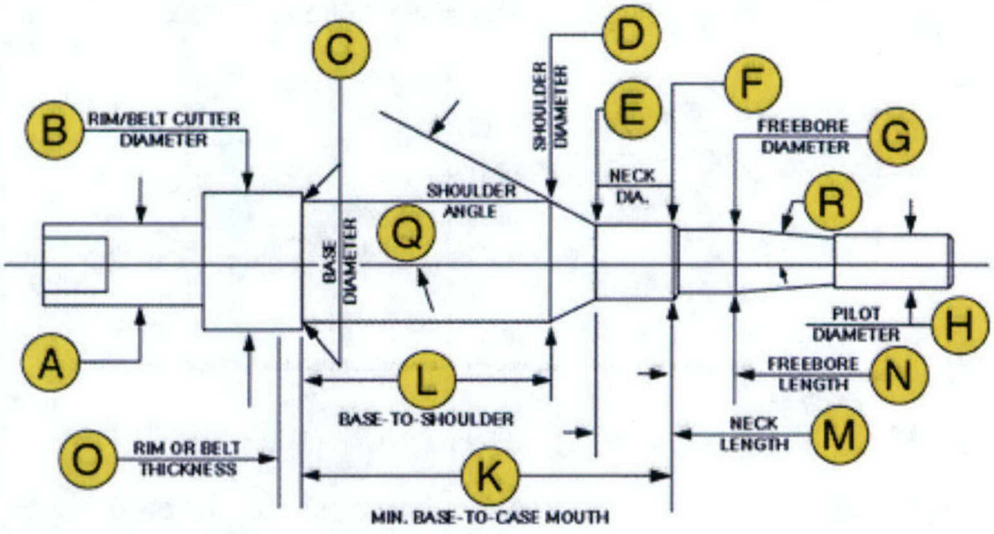

Figure 5
2.5 deg half angle forcing cone modified 7.62-mm chamber reamer key

Table 1
2.5 deg forcing cone reamer dimensions

Dimension key	Dimension (in.)
A:	0.4370
C:	0.474
D:	0.4570
E:	0.3460
F:	0.3440
G:	0.30850
H:	(TBD, est.0.2897 in.)
K:	2.0250
L:	1.3560
M:	0.3300
N:	0.1200
O:	0.2000
Q:	20 degree
R:	2 1/2 degree

The machining sketch for the polygonal barrel is shown in figure 6.

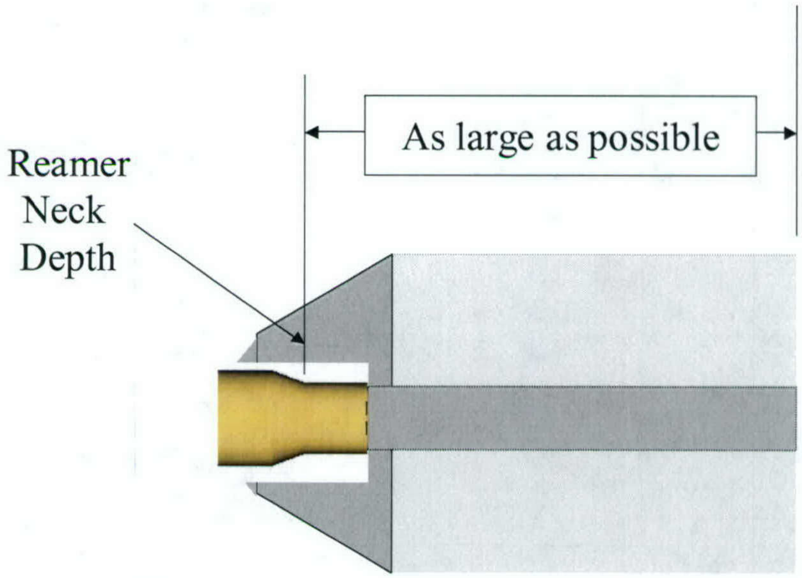

Figure 6
Polygonal barrel (barrel 3) machining sketch

The 2.5 deg half angle forcing cone reamer was used to put a forcing cone into the polygonal barrel.

The engraving force for each configuration was tested at the University of Vermont (UVM) mechanical and civil engineering lab. Since the barrel sections did not have identical exterior configurations, Brian Esser, a graduate student at UVM, designed adapters to hold each barrel section for the push test. Figure 7 shows the barrel sections and the adapters.

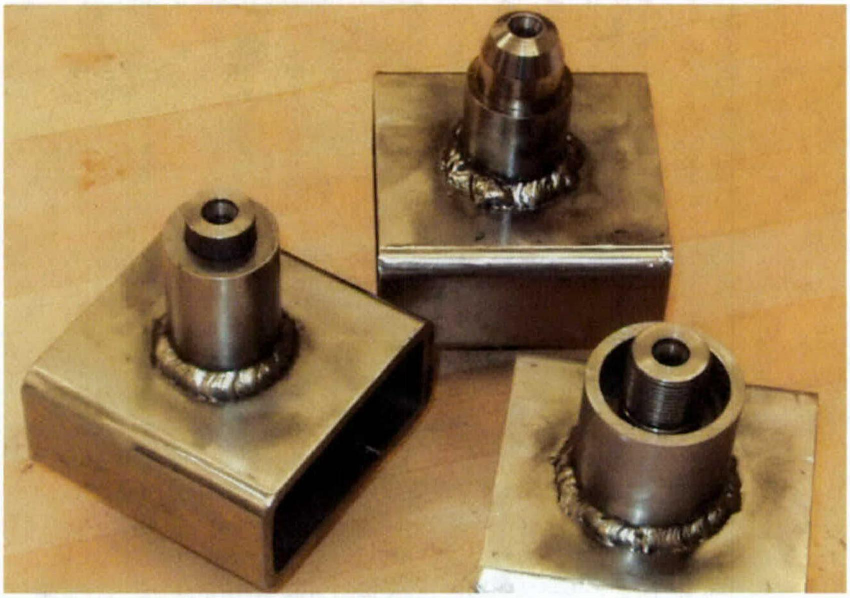

Figure 7
Test barrel sections and fixture adapters

Each barrel section was approximately 2.5 in. in length, allowing push force measurements over approximately 45 mm. In figure 7, the baseline M240 barrel section (barrel 1) is shown in the lower right hand corner, the M240 barrel section with a 2.5 deg half angle forcing cone (barrel 2) is shown on the left hand side, and the polygonal barrel section with the 2.5 deg half angle forcing cone is shown at the upper right side; each with their respective adapters.

The push test machine set up is shown in figure 8. For this test, the cross head speed was set at 100 mm/s, and the required push force (N) as a function of travel was recorded electronically.

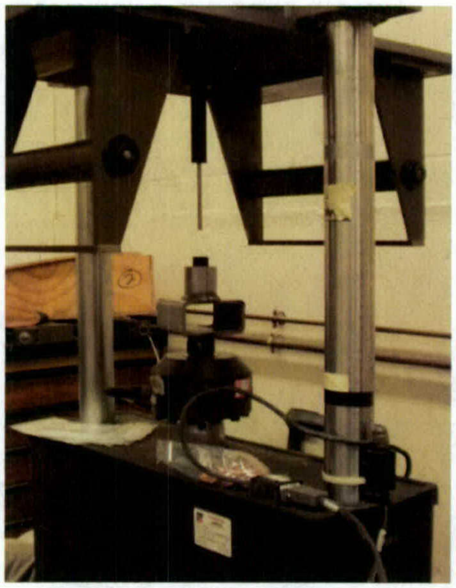

Figure 8
UVM push test machine set-up

In examining the push force data, along with the barrel sections and initial projectile seating depths, it was evident that the test data captures the initial push force to peak engraving, but the decay from peak was artificial. The length of the barrel section chosen for push testing was chosen by elastic column buckling considerations for a reasonable punch length. For this reason, the push test data was fairly consistent in end travel, and the reader should use the data contained herein with caution. However, for most interior ballistics simulations, the travel at peak engraving force extends well beyond the travel at peak pressure, ensuring the results obtained by using the measured data should be reasonably accurate.

A close-up of the barrel test section, the barrel adapter, the push punch, and the test cross head is shown in figure 9.

Figure 9
Polygonal barrel sample push testing

Standard 7.62 mm production M80 projectiles and Barnes 30 caliber, 150 grain, XFB solid copper projectiles (commercially available) were used for this test. A cross-section of the M80 projectile is shown in figure 10, with the Barnes "X" bullet cross-section shown in figure 11.

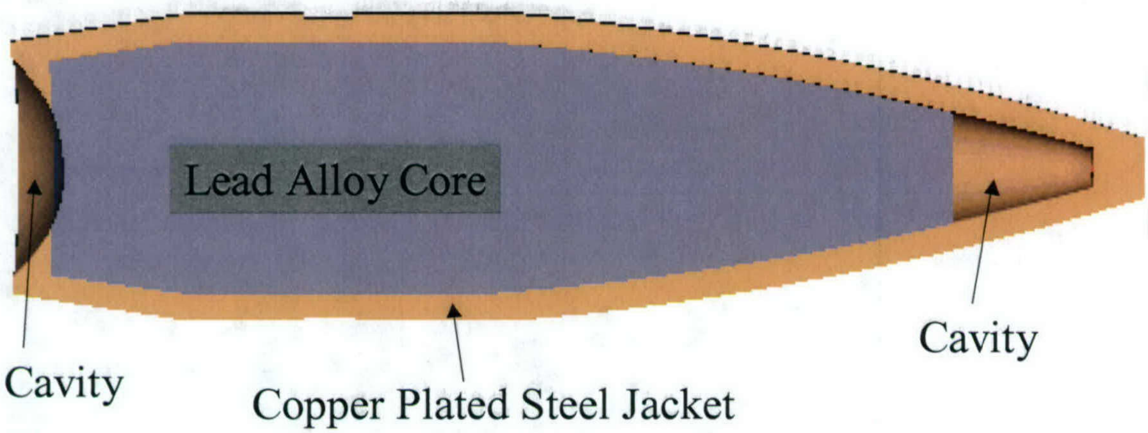

Figure 10
7.62 mm M80 projectile

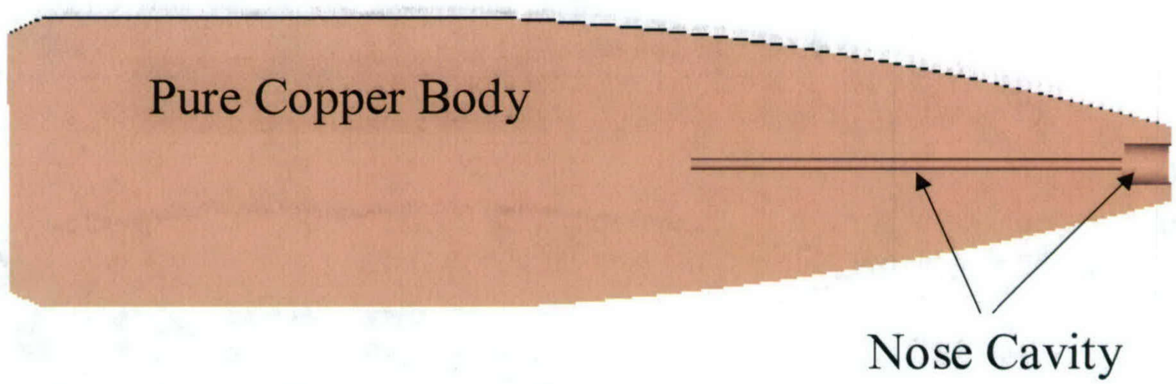

Figure 11
Barnes 30 caliber 150 grain XFB projectile

RESULTS

The push force versus travel was recorded for each barrel test section. The results are listed next for each barrel.

M240 Baseline

The average push test forces versus travel for the baseline M240 barrel is shown in figure 12.

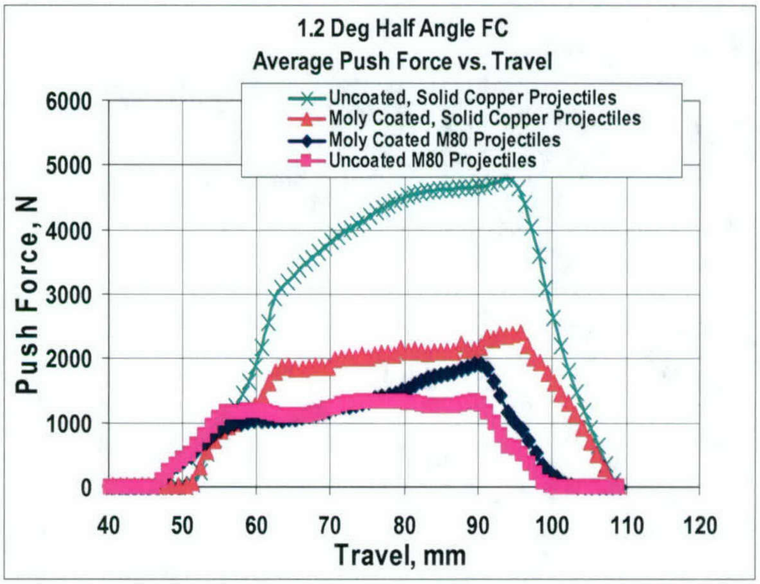

Figure 12
M240 barrel, average push force versus travel and bullet type

As is evident in figure 12, the resistance force versus travel is quite different for the M80 projectile (with a lead core) versus the solid copper core Barnes "X" projectile. Also shown is the effect of an after market, spray-on molybdenum lubricant on resistance force for both bullet types.

In simulating interior ballistics performance, it is usually more convenient to express the projectile resistance force as an equivalent pressure, which can be subtracted from the chamber pressure to determine the net force operating on the projectile. This is done by dividing the push force by the bore area to obtain a pressure, expressed as pounds per square inch in English units or megapascals (MPa) in SI units. Figure 13 shows the data presented in figure 12 expressed as a pressure.

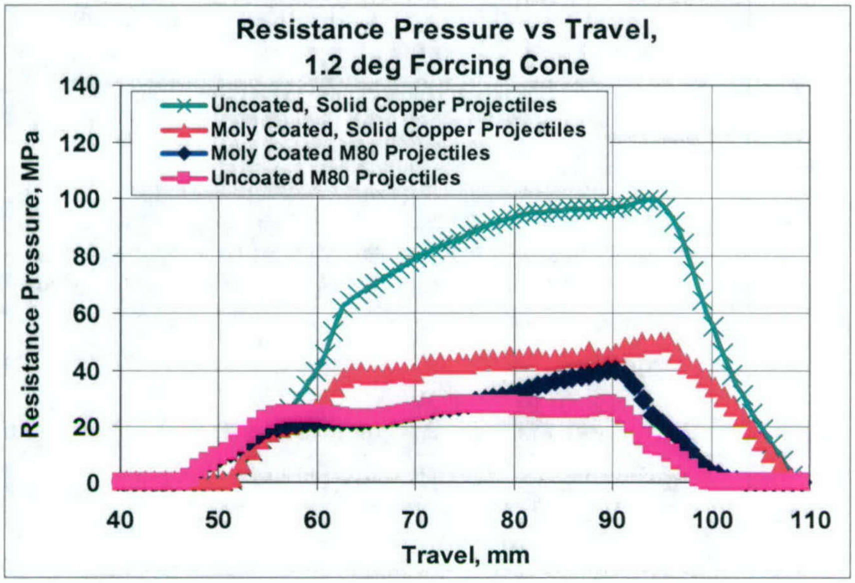

Figure 13
M240 barrel, resistance pressure versus travel and bullet type

One of the interesting observations made during the push test was the failure of 15 test projectiles to achieve a reasonably consistent push force value. Figure 14 shows the peak push force value attained for the M240 barrel with the 1.2 deg half angle forcing cone for various bullets and lubrication conditions.

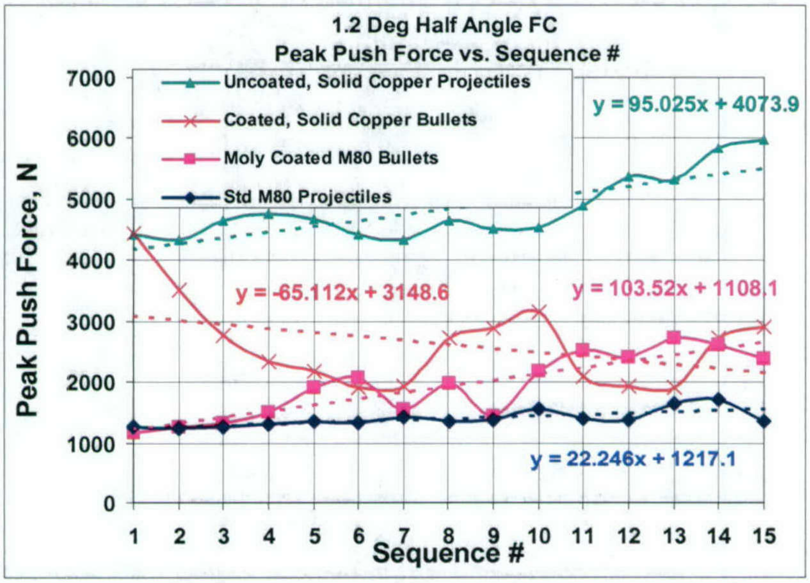

Figure 14
M240 barrel, push force versus sequence number and bullet type

With the exception of the coated Barnes "X" bullet, which shows a decreasing trend with each projectile pushed through the standard M240 barrel, all tested projectiles exhibited an increase in peak resistance force with increasing number of projectiles pushed through the barrel. The failure to attain some reasonably consistent peak push force within 15 samples was a bit of a surprise, but can perhaps be explained by the low number of projectiles transitioning through the barrel.

The standard deviation of push force may be responsible for a large portion of the interior ballistic variability observed during normal firing and lot acceptance testing for small caliber ammunition. Figure 15 shows the standard deviation in push force as a function of travel for the baseline M240 barrel with both projectiles and both lubrication conditions.

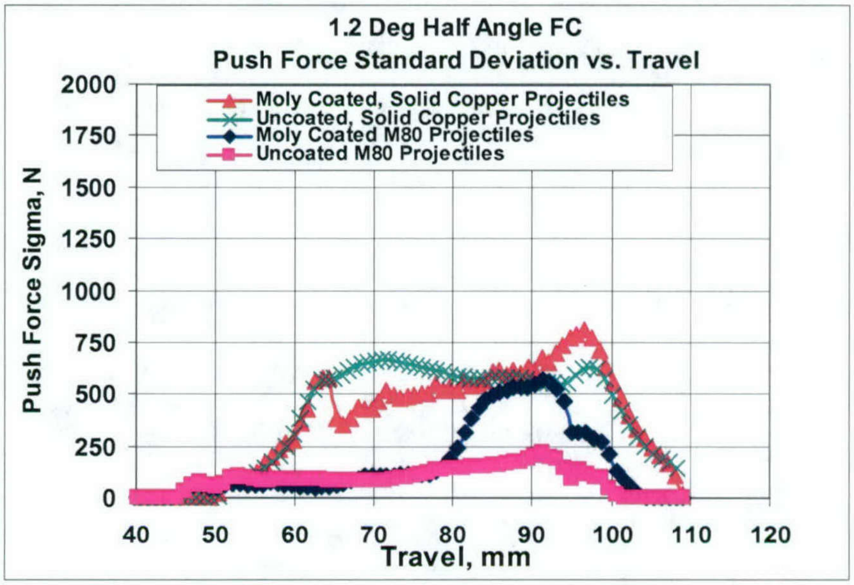

Figure 15
M240 barrel, push force standard deviation versus travel and bullet type

An increase in push force standard deviation near the end of the forcing cone is expected as any variability in engraved length of projectile results in some projectiles exhibiting large push force values while others have very low push force values.

The push force standard deviation as a percent of the mean measured push force is shown in figure 16.

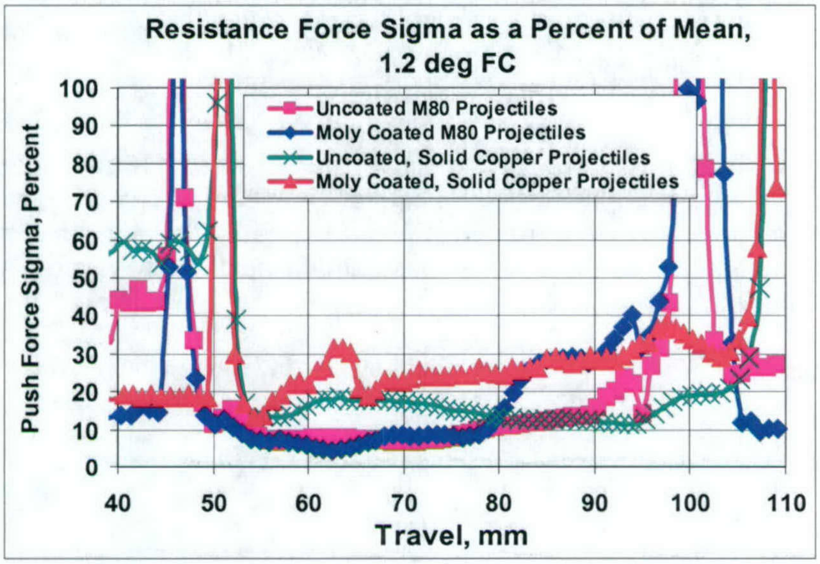

Figure 16
Resistance force standard deviation percent versus travel and bullet type

Figure 16 shows wide variability in push force standard deviation at either end of the push force travel for two reasons. Early in the in bore travel, the push force is quite low, so small differences in push force result in large percent push for standard deviations. At the end of travel, the reason for increased variability has already been discussed.

The individual push test results for the uncoated M80 projectiles in the M240 barrel are shown in figure 17.

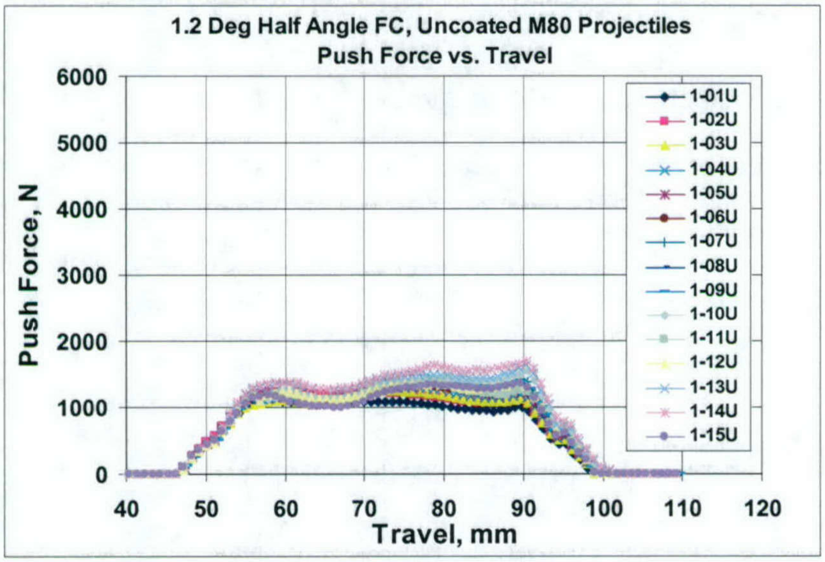

Figure 17
M240 barrel, uncoated M80 projectile, individual push test results

The push force behavior for the uncoated M80 projectiles in the baseline M240 barrel was fairly consistent, despite the trend for increasing push force values with increasing numbers of projectiles pushed through the bore.

Figure 18 shows the individual push force values for moly coated M80 projectiles in the baseline M240 barrel. As shown, there is a significant increase in push force, especially late in the forcing cone, exhibited by the projectiles pushed late in the test. This may indicate deposition of molybdenum lubricant on the forcing cone. Whether this lubricant can or would be removed by the high temperature, high velocity gases that would be present during actual firing have not been determined.

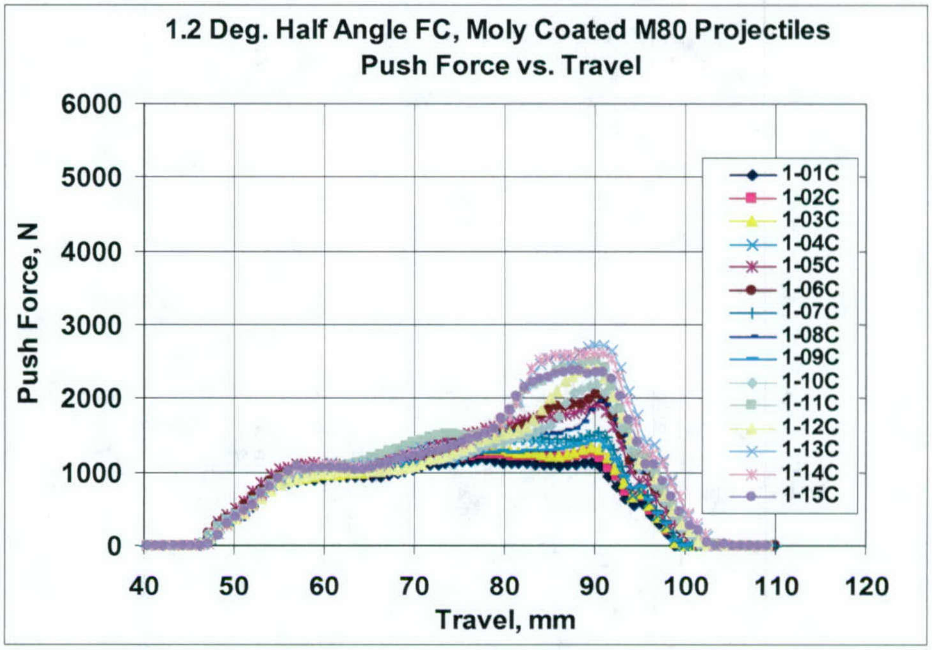

Figure 18
M240 barrel, moly coated M80 projectiles, individual push test results

Figure 19 shows the individual push force values for the Barnes "X" bullets as a function of travel. As previously described, there is a trend towards increasing push force values as the test progressed.

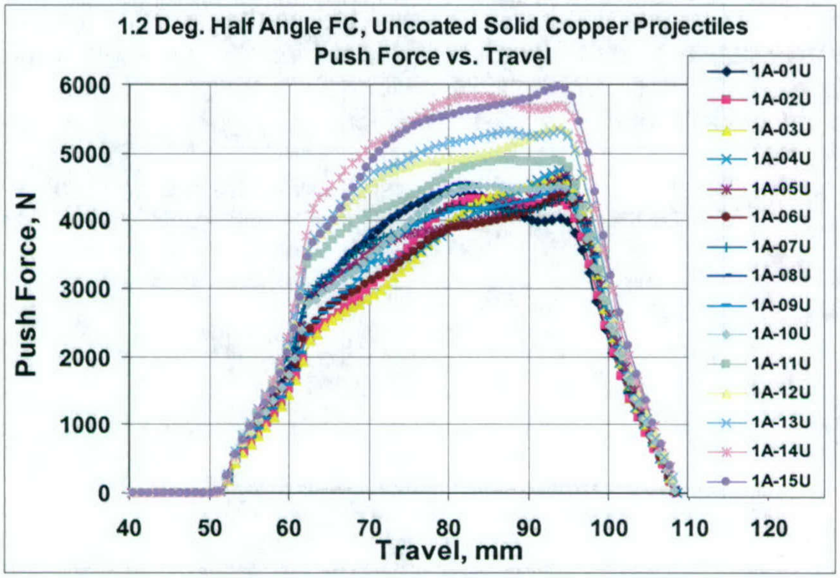

Figure 19
M240 barrel, uncoated Barnes "X" projectile, individual push test results

Figure 20 shows the individual push force values for the Barnes "X" bullets as a function of travel. Contrary to previous push force testing, there is a general trend towards decreasing push force values as the test progressed.

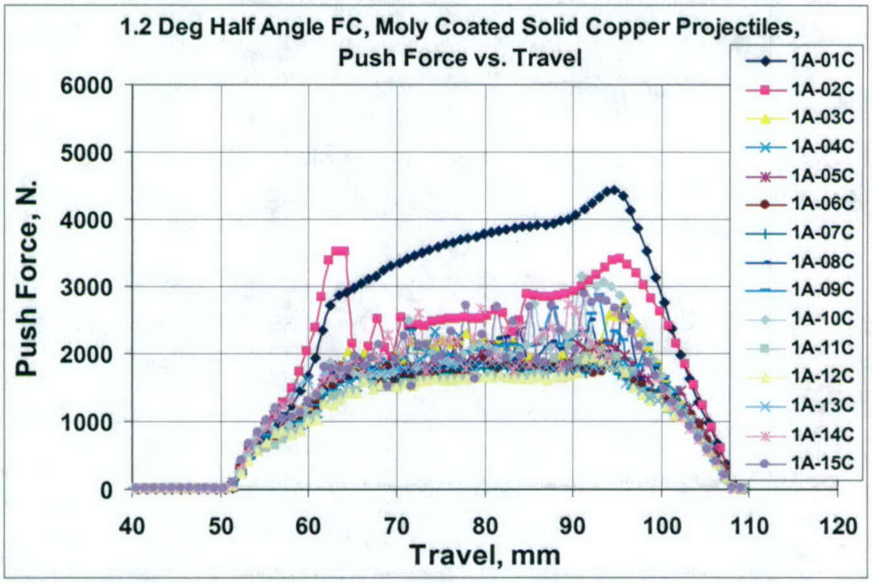

Figure 20
M240 barrel, moly coated Barnes "X" projectiles, individual push test results

M240 with Modified Forcing Cone

One of the design variables assessed for this study is the effect of forcing cone angle on push force. It was initially expected that an increase in forcing cone angle would result in an increase in push force, but that trend was not exhibited in testing. A more complete discussion of this phenomenon is made in the Discussion section.

Figure 21 shows the average push force versus travel for bare and moly coated M80 projectiles in a section of M240 barrel with a 2.5 deg half angle forcing cone.

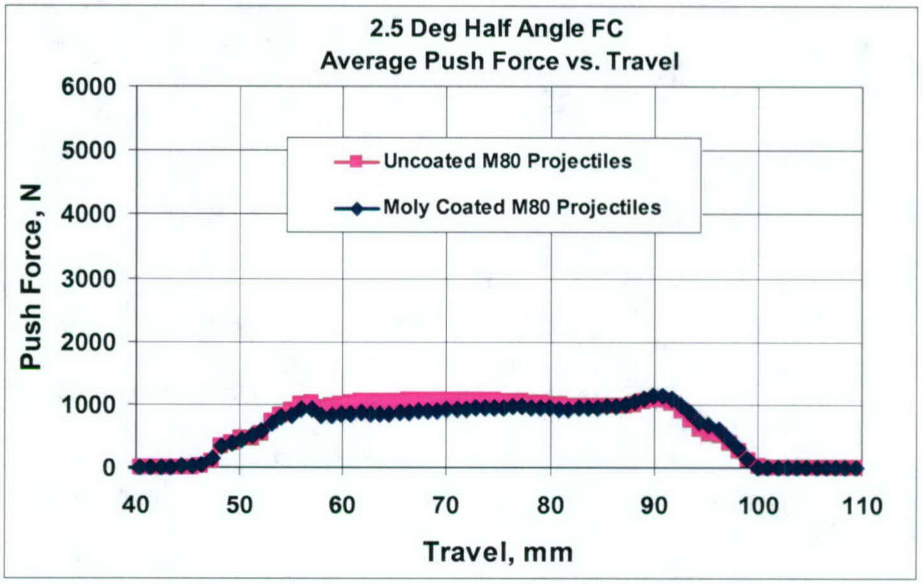

Figure 21
2.5 deg half angle mod M240 barrel, average push force versus travel and bullet type

Figure 22 shows the resistance pressure versus travel for M80 projectile with and without lubrication in the baseline M240 barrel with a 1.2 deg half angle forcing cone and a section of M240 barrel with a 2.5 deg half angle forcing cone.

Figure 22 also shows an increased average resistance pressure exhibited by the 1.2 deg half angle forcing cone. This is an unexpected result, and is more fully explored in the Discussion section.

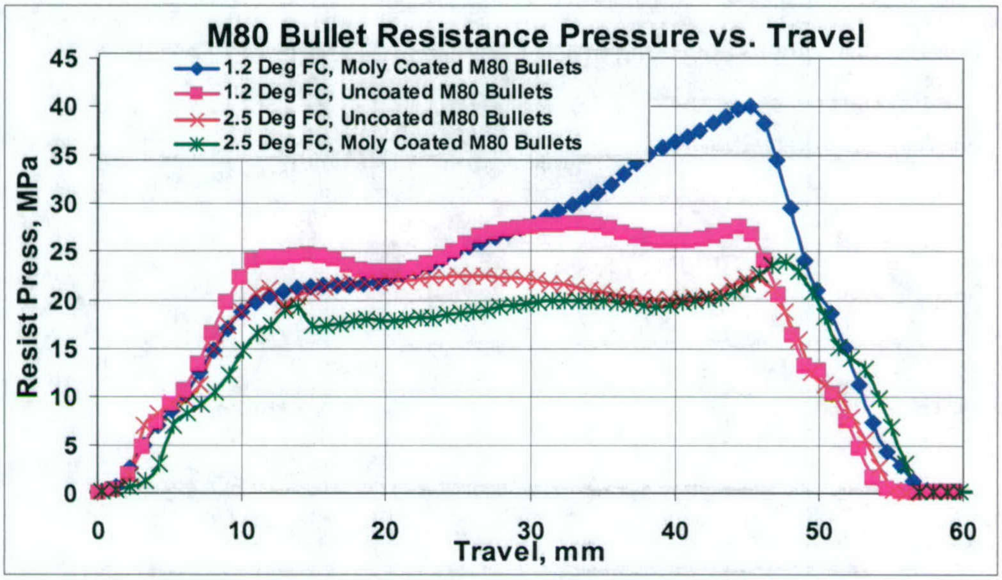

Figure 22
M80 resistance pressure versus travel, forcing cone angle, and lubrication

Figure 23 shows the standard deviation in push force for bare and lubricated M80 projectiles in the modified M240 barrel with a 2.5 deg half angle forcing cone. For this barrel configuration, a decrease in push force standard deviation is seen with molybdenum coating.

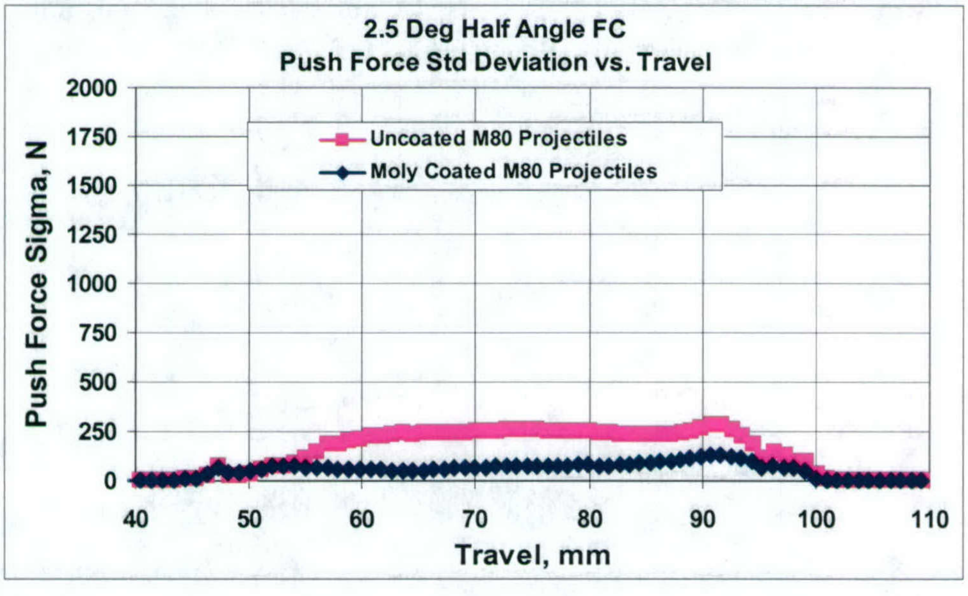

Figure 23
2.5 deg half angle mod M240 barrel, push force standard deviation versus travel and bullet lubrication

Figure 24 shows the peak push force as a function of test number for the 2.5 deg half angle forcing cone for the bare and lubricated M80 projectiles. The lowest slope of peak push force versus sequence number observed in this test occurs with the lubricated M80 projectiles in the 2.5 deg half angle forcing cone.

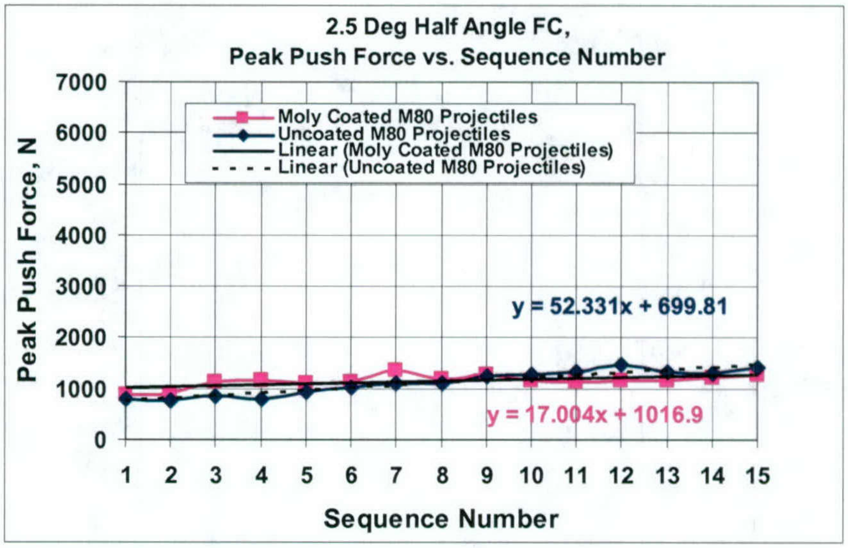

Figure 24
2.5 deg half angle mod M240 barrel, push force versus sequence number and bullet type

Polygonal Barrel

The polygonal barrel push tested for this assessment was a heptagonal barrel designed under the previous study contract. The cross-section is shown in figure 25.

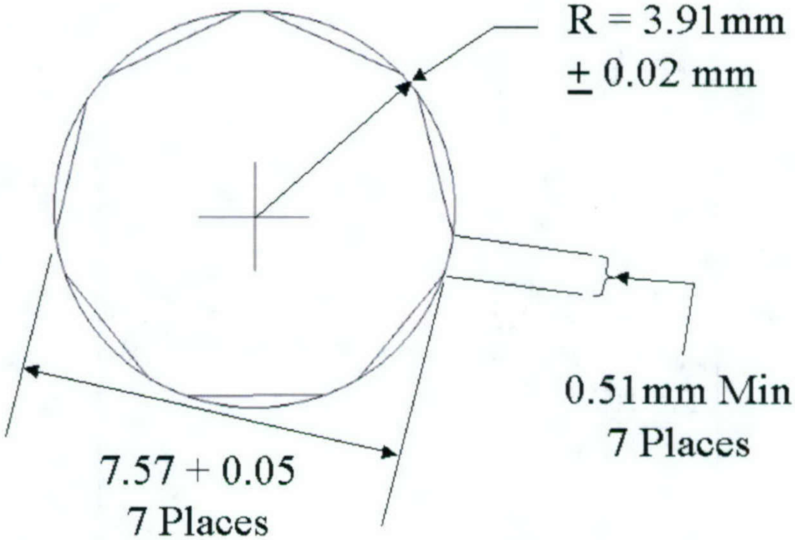

Figure 25
Heptagonal barrel section definition

The heptagonal barrel provided had no forcing cone, so the 2.5 deg half angle chamber reamer made for the M240 barrel section was used. A 2.5 in. long section of barrel was cut off the muzzle for the push test barrel sample, and a partial chamber including the forcing cone was machined into the sample.

Figure 26 shows the average push force for bare and lubricated M80 projectiles in the heptagonal barrel with the 2.5 deg half angle forcing cone.

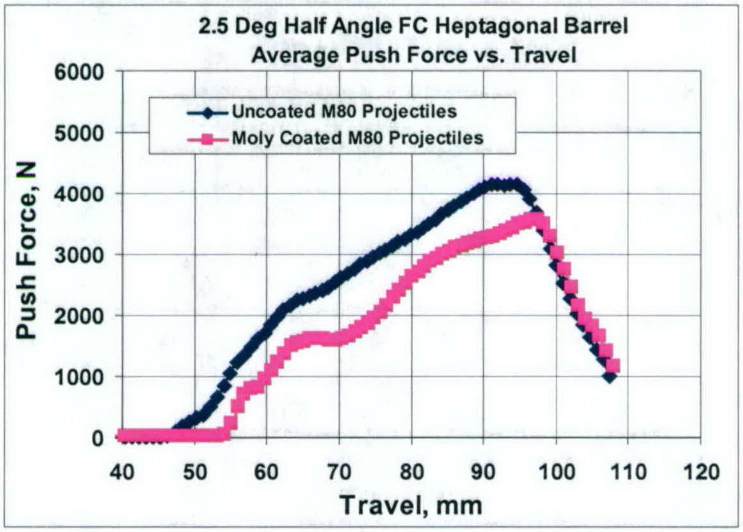

Figure 26
Heptagonal barrel average push force versus travel and bullet type

Figure 27 shows the push force standard deviation as a function of travel for bare and lubricated M80 projectiles in heptagonal barrel with a 2.5 deg half angle forcing cone.

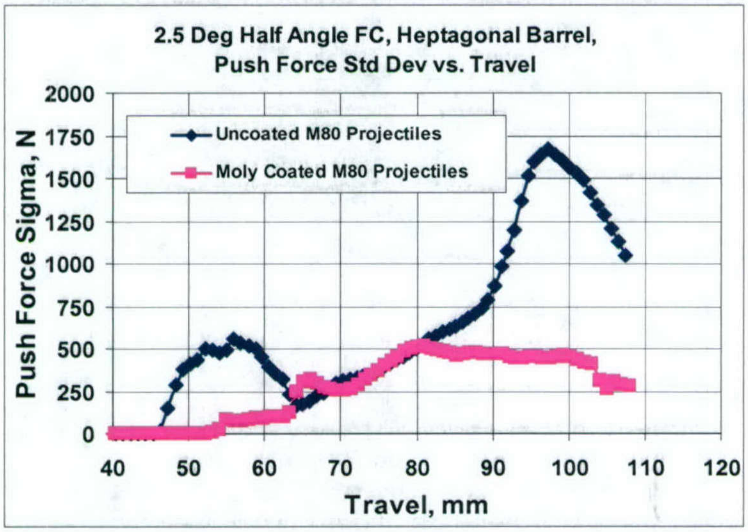

Figure 27
Heptagonal barrel push force standard deviation versus travel and bullet type

Figure 27 also shows significantly reduced push force standard deviation for the lubricated M80 projectiles early and late in the push test. The reduction in standard deviation early in travel was due to a more consistent push force start location for the lubricated projectiles compared to the unlubricated projectiles. Variability in push force start location for the unlubricated projectiles is shown in figure 28.

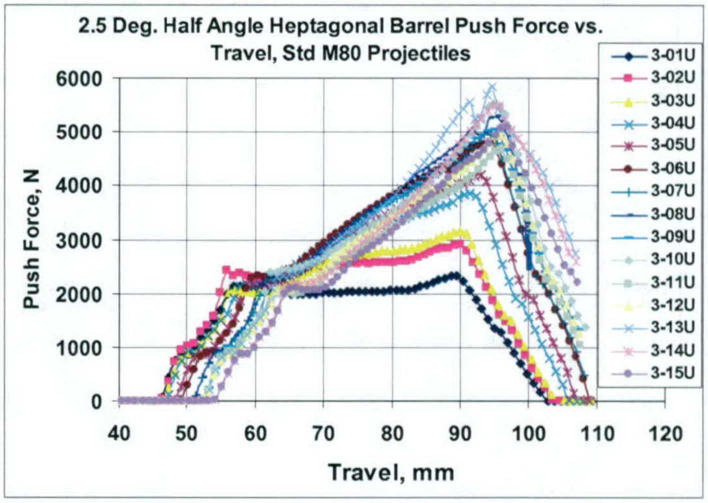

Figure 28
Heptagonal barrel, uncoated M80 bullets, individual push force measurements

The origin of the push force start variability may be due to wear of the forcing cone material. Increased push force late in the forcing cone may be due deposition of bullet or forcing cone material.

Figure 29 shows the individual push force versus travel measurements for the molybdenum coated projectiles in the heptagonal barrel with a 2.5 deg half angle forcing cone.

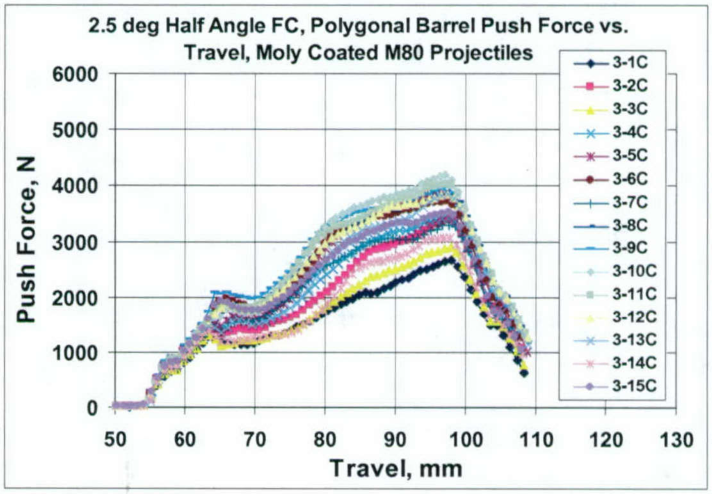

Figure 29
Heptagonal barrel, moly coated M80 bullets, individual push force measurements

Figure 30 shows the peak engraving force versus sequence number for lubricated and unlubricated M80 projectiles pushed through the heptagonal barrel section with a 2.5 deg half angle forcing cone. As with the 2.5 deg forcing cone modified M240 barrel, lower push forces and shallower slope with increasing sequence number was observed with lubricated M80 projectiles.

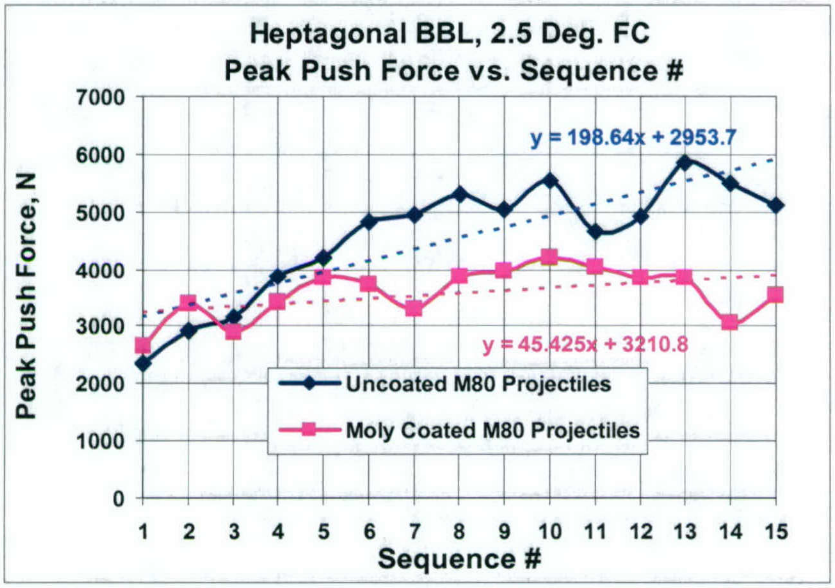

Figure 30
Heptagonal barrel, push force versus sequence number

An attempt was made to push solid copper Barnes "X" bullets through the heptagonal barrel, but the peak push force rose to unacceptably high values. Plastic column buckling of the push rod brought the push test to an abrupt end.

DISCUSSION

Projectile Construction

With the push test nearly complete, the observed resistance forces for the M80 bullets did not match the expected resistance forces very well. It had been assumed that minor modifications of an empirically determined resistance (force) pressure model developed for medium caliber projectiles by J. Wolf and G. Cochran in the 1970's could accurately estimate the resistance force for a particular projectile/barrel configuration (table 2). The empirically determined resistance pressure model for medium and large caliber projectiles is:

$$P_r = \frac{P_{rN} * (BD - 1.0) * (BL) * (FF) * (1.92/(G/L)Ratio) + K)}{Cos\, \Theta/2} \qquad (1)$$

where

P_r	= Computed resistance pressure
P_{rN}	= Normalized resistance pressure
BD	= Band diameter, calibers
BL	= Band length, calibers
FF	= Material code, 1.0 for Fe and Cu, 0.2 for plastics
K	= Small residual constant
Θ	= Forcing cone angle

Table 2
Normalized resistance pressure versus band length

P_{rN} (psi)	P_{rN} (MPa)	Travel, band lengths
2000	13.8	0.0
15000	103.4	0.2
15000	103.4	0.8
10000	69.0	1.0
7000	48.3	1.5
4000	27.6	4.0
2500	17.2	10.0
2000	13.8	30.0
1500	10.3	60.0
1500	10.3	2000.0

Equation 1 assumes the projectile has a defined rotating band that is an interference fit with both the lands and grooves of the barrel. Small caliber projectiles are manufactured using forming dies to plastically deform the projectile exterior, thus controlling their finished diameter. The finished diameter can be from a slight clearance to a slight interference with the barrel groove, but it is always an interference fit with the land diameter of the barrel.

Equation 1 was modified to estimate the resistance pressure of body engraved projectiles. The modified equation is

$$P_r = \frac{P_{r(ref)} * (BandDia - 1.0) * Bandlength * BandMat'lFF * StiffnessFF}{16.9 * Cos\frac{\theta}{2} 8 G/_{L} Ratio} + K \qquad (2)$$

where

P_r	= Computed resistance pressure
$BandDia$	= Band diameter, calibers
$BandLength$	= Band length, calibers
$Mat'lFF$	= Material code, 1.0 for Fe and Cu, 0.2 for plastics
$StiffnessFF$	= Stiffness factor from chart
K	= Small Residual Constant

Table 3
Small caliber reference resistance pressure versus travel

P_{rN} (psi)	P_{rN} (MPa)	Travel, band lengths
2000	13.8	0.00
372650	2570.0	1.4 FC Len*
478500	3300.0	(4.74 + FC Len)/2
507500	3500.0	4.0 FC Len
5400	37.2	4.8 + FC Len
5400	37.2	8.00
5400	37.2	10.00
5400	37.2	30.00
5400	37.2	60.00
5400	37.2	2000.00

*FC Len = Forcing cone length

All resistance pressure factors are identified in table 3. The modifications to equation 1 to account for change in projectile diameter were based on the result of firings conducted at Federal Cartridge Company.

Thus, when initial resistance force measurements were considerably lower than expected, it was hypothesized that they were a function of the specific construction of a given projectile. Specifically, it was believed that the elastic modulus of the projectile components and their relative diameter at the forward and aft bourrelets affected the measured engraving force. The push test was expanded to include the pure copper Barnes "X" bullets, conclusively proving that the projectile construction does indeed significantly affect resistance force (fig. 12). The resistance force measured for the uncoated Barnes "X" bullets in the baseline M240 barrel is significantly higher than for the uncoated M80 projectiles (by a factor of approximately 3:1) for the travel between 55 mm and 90 mm. The presence of external lubrication reduces the increase in resistance pressure to a factor of 1.5:1 for the Barnes "X" bullet.

In an attempt to quantify the effect of relative radial stiffness on resistance force (pressure), a modified "strength of materials" approach was used to estimate the absolute radial stiffness for composite projectiles. The results of this computation were then scaled based on the diameter of the "interface" (core diameter/projectile diameter) and a composite radial stiffness was computed using the following relation

$$K_T = \left(\frac{1}{K_{interior}} + \frac{1}{K_{exterior}} \right)^{-1} + K_{interior} + K_{exterior} \tag{3}$$

where

K_T = Total radial stiffness

$K_{interior}$ = Computed radial stiffness of the interior "core"

$K_{exterior}$ = Computed radial stiffness of the exterior "shell"

Figure 31 shows the result of the computations made to generate "absolute" radial stiffness numbers using the relationship in equation 3.

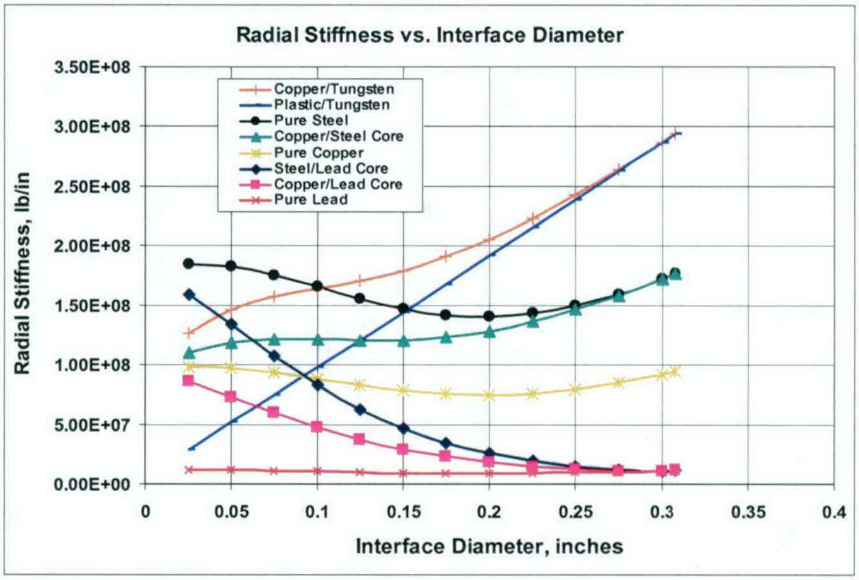

Figure 31
Radial stiffness versus interface diameter and material

While the ability to compute the radial stiffness is interesting, it is far more useful from a computational standpoint to compute the relative radial stiffness as the resistance force is proportional to the square root of the relative radial stiffness. Figure 32 shows the relative radial stiffness of projectiles of varying construction as a function of the interface diameter (in calibers) assuming the relative radial stiffness of a pure steel projectile = 1.0, along with some polynomial equations to estimate the relative radial stiffness.

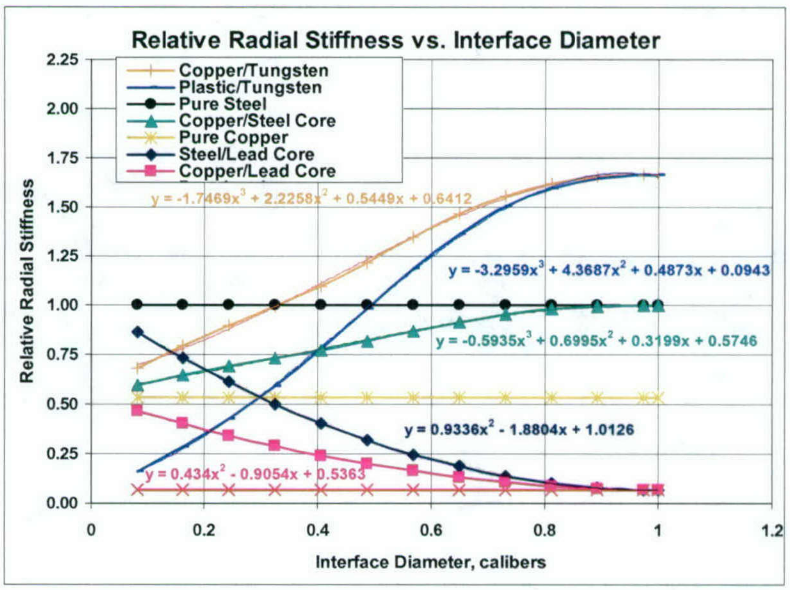

Figure 32
Relative radial stiffness versus interface diameter in calibers

Figure 32 shows the relative radial stiffness of composite projectiles as a function of interface diameter expressed in calibers. For the effect of radial stiffness on resistance pressure, the square root of the factor determined in figure 32 must be taken. The relative resistance pressure factor is shown in figure 33.

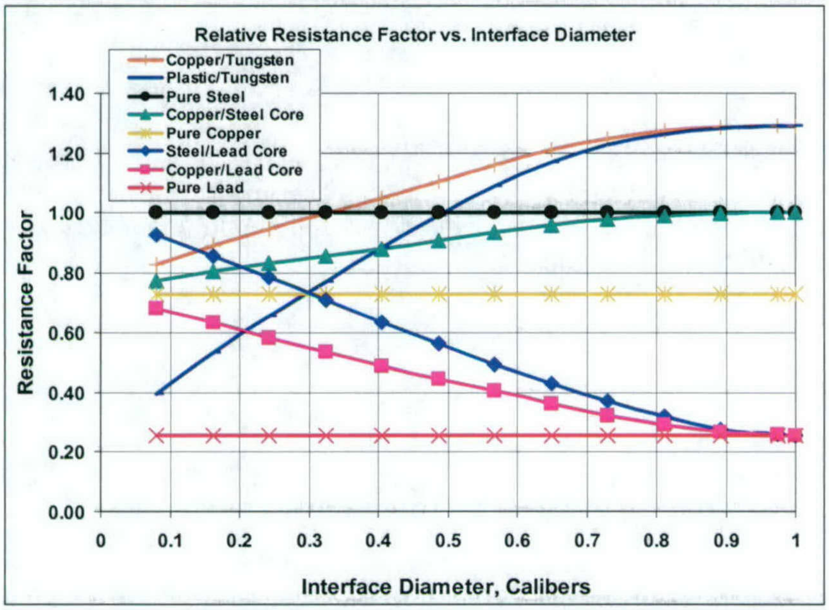

Figure 33
Relative resistance factor versus interface diameter in calibers

Using equation 2 and table 3, the resistance pressure versus in bore travel can be computed as a function of projectile construction. A comparison between the predicted and measured resistance pressure is shown in figure 34.

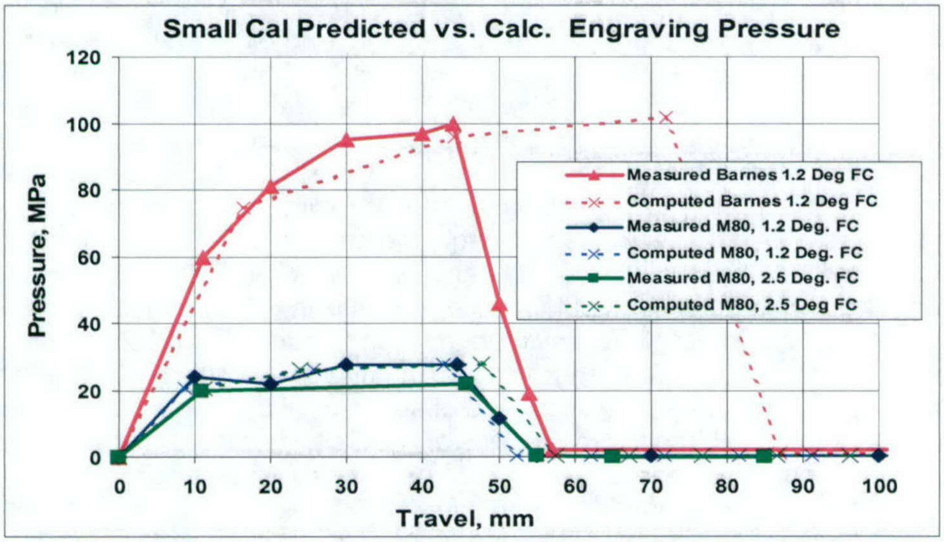

Figure 34
Comparison of predicted versus measured resistance pressure versus travel

As shown in figure 34, the resistance pressure versus travel for the M80 projectile in the baseline and 2.5 deg forcing cone half angle shows reasonable agreement between measured and predicted data. For the Barnes "X" bullet, however, there is considerable disagreement regarding the travel. The measured resistance force travel was short because of the limited punch length needed to prevent elastic column buckling of the punch as the projectile was pushed through the barrel test section.

Forcing Cone Angle

As shown in equations 1 and 2, the forcing cone angle has previously been shown to affect resistance pressure. The basis of this effect was assumed to be the von Mises stress elastically imposed on an inclined surface. Equation 4 shows the von Mises yield criteria for materials with combined loading conditions.

$$2\sigma^2 = (\sigma_1 - \sigma_2)^2 + (\sigma_1 - \sigma_3)^2 + (\sigma_2 - \sigma_3)^2 \tag{4}$$

where

σ_1 = Principal axis stress (longitudinal)
σ_2 = Principal axis stress (radial)
σ_3 = Principal axis stress (hoop)
σ = Combined stress

In assessing the von Mises yield criteria, an increase in total stress should occur on the projectile with increasing forcing cone angles. However, in analyzing the resistance pressure versus travel force for small caliber bullets, it is evident that there are different engraving mechanisms in play as a function of forcing cone angle.

Figure 35 shows the average force versus travel measurement for the 1.2 deg half angle forcing cone (standard M240) and the 2.5 deg half angle forcing cone (modified M240 barrel) for uncoated and moly coated M80 bullets. It is evident in figure 35 that lower resistance forces were measured with the higher forcing cone angle, opposite of what was expected. This indicates that for the more shallow forcing cone angle, the engraving process was more "elastic", resulting in higher stresses between the bullet and the barrel. The higher bullet-barrel stresses caused higher push forces, to the point that the increase in projectile diameter caused by the presence of spray-on molybdenum lubrication actually increases the push force late in the engraving process. With the increased forcing cone angle of 2.5 deg half angle, there is apparently a reduction in residual elastic stress between bullet and the barrel, resulting in lower push forces regardless of the presence of lubrication. This is interesting, as it indicates the existence of some forcing cone angle at which engraving forces peak, and above which the resistance force decreases. This peak engraving force cone angle must lay between 1.2 deg and 2.5 deg half angle for the M80 projectile. The observation that the resistance force is nearly constant for lubricated and unlubricated projectiles at a 2.5 deg forcing cone half angle indicates that guns with this forcing cone angle should exhibit reduced muzzle velocity variability. There is also a reduced standard deviation in push force for the 2.5 deg forcing cone half angle compared to the 1.2 deg forcing cone. At the end of the forcing cone, an increase in push force standard deviation would be expected as variability in the engraved projectile length should result in increased force variability. Push force standard deviation versus travel for unlubricated and lubricated M80 bullets in a 1.2 deg forcing cone and 2.5 deg forcing cone is shown in figure 36.

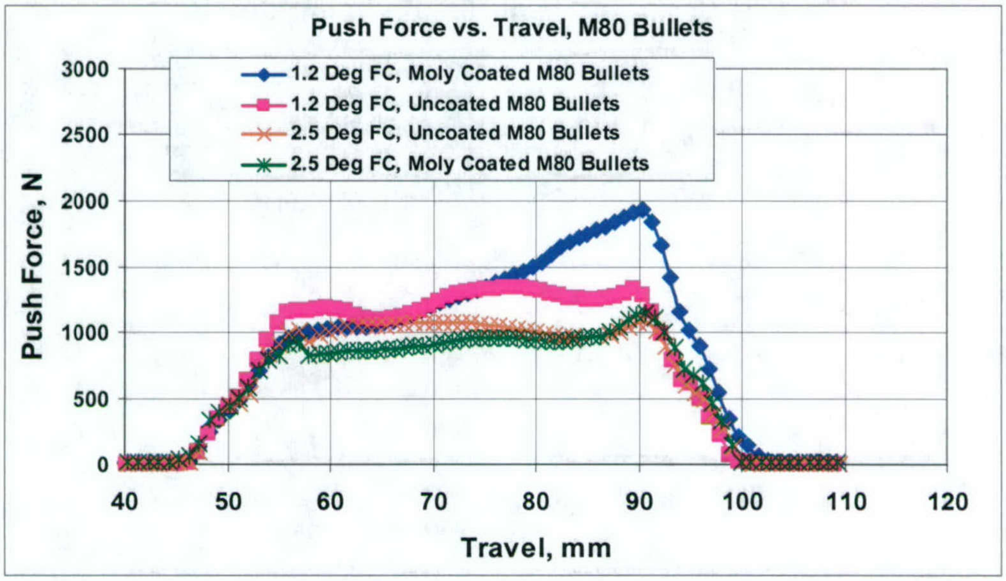

Figure 35
Engraving force versus travel for M80 bullets with two forcing cone angles, coated and uncoated

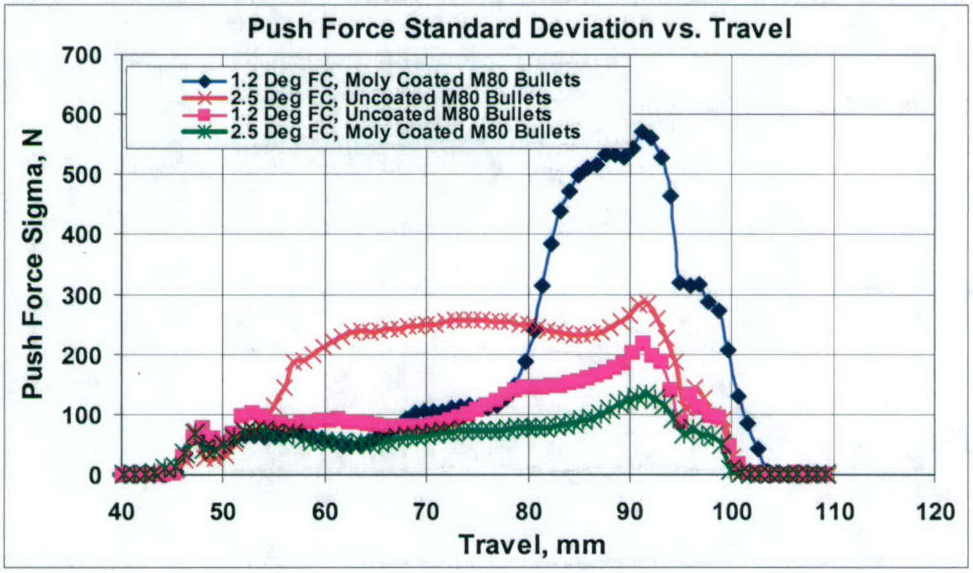

Figure 36
Push force standard deviation versus travel and forcing cone half angle

Interior Ballistic Simulations

Variability in projectile engraving resistance can have a fairly dramatic effect on the peak pressure generated by the propellant. However, variability in peak pressure does not necessarily linearly translate into muzzle velocity variability. Figure 37 shows the effect of barrel and forcing cone configuration on the expected peak pressure for uncoated M80 projectiles in each of the test barrels.

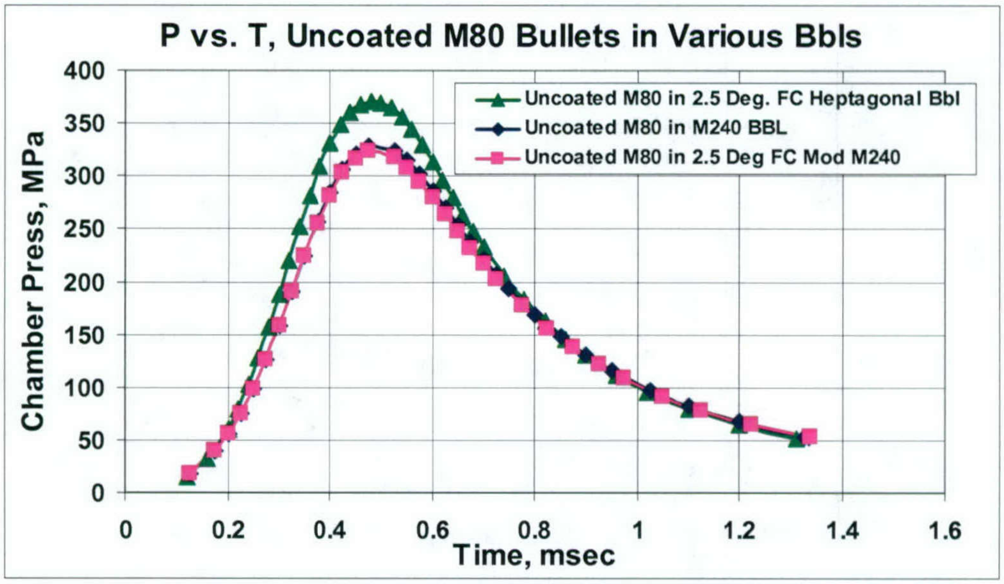

Figure 37
Predicted pressure versus time for bare M80 bullets in tested barrels

As shown in figure 37, the difference in peak pressure between the 1.2 deg and 2.5 deg half angle forcing cone is quite small. The increase expected for the heptagonal barrel is due primarily because of the increase in resistance force (pressure) early in the in bore travel. Increases in resistance pressure that occur after peak pressure has occurred do not affect the peak chamber pressure. This effect is shown in figure 38.

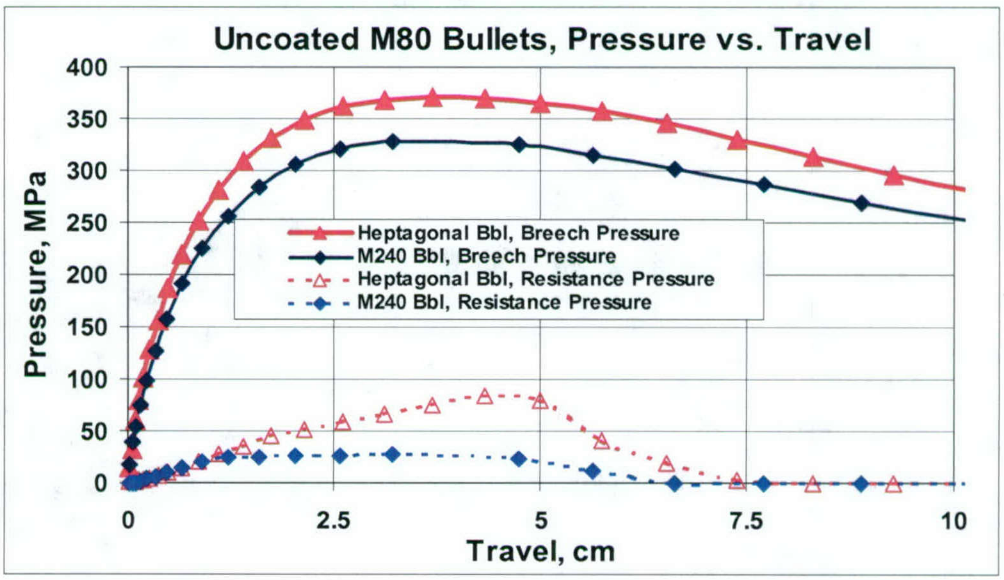

Figure 38
Chamber and resistance pressure versus travel for bare M80 projectiles

Early in the interior ballistic cycle, the rate of volume generation as a result of projectile travel strongly influences the peak chamber pressure achieved by a cartridge. To this end, projectile/barrel/forcing cone combinations that exhibit increased resistance to initial projectile movement also exhibit increased peak chamber pressure. Figure 38 shows the effect on peak chamber pressure caused by the nearly double resistance pressure before peak chamber pressure is achieved. The relative insensitivity of peak chamber pressure (+15%) to large changes in resistance pressure (+100%) was unexpected, and may be due to the linear burn rate versus depth burned propellant deterrent model used in the modified Baer-Frankle interior ballistics simulation used.

Figure 39 shows the predicted chamber pressure versus time for molybdenum coated M80 bullets in the three test barrel sections.

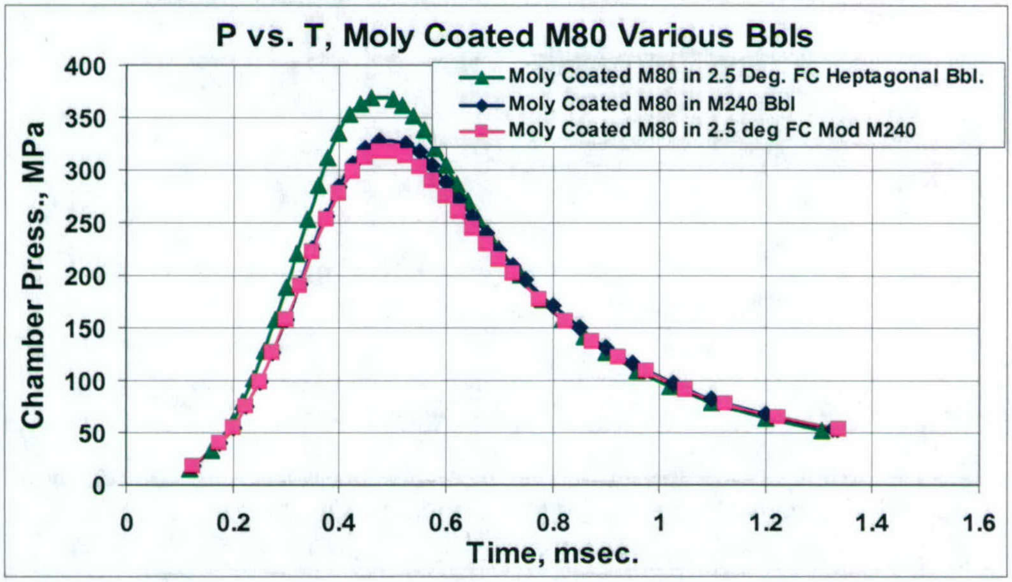

Figure 39
Predicted pressure versus time for moly coated M80 bullets in test barrels

REVISED POLYGONAL BARREL CONFIGURATION

Given the unexpected increase in resistance pressure observed with the recommended heptagonal barrel configuration, the design was revised to reduce the engraving pressure. Comparing the original polygonal design to the revised design, the revised design has corner width twice the original width. The dimensional details of the revised heptagonal barrel are shown in figure 40. The revisions to the flat length make the bore area of the heptagonal barrel equal to 99.4% of the baseline M240 barrel. This makes the expected average engraving force for the M80 projectile through this barrel approximately 20 to 25% higher than the baseline barrel. Given the previous simulations, the increase in average engraving force is expected to have only minor effect (2 to 4 kpsi) on peak pressure generated by inventory projectiles. Some "finessing" of the forcing cone angle and free run is likely to reduce that number further.

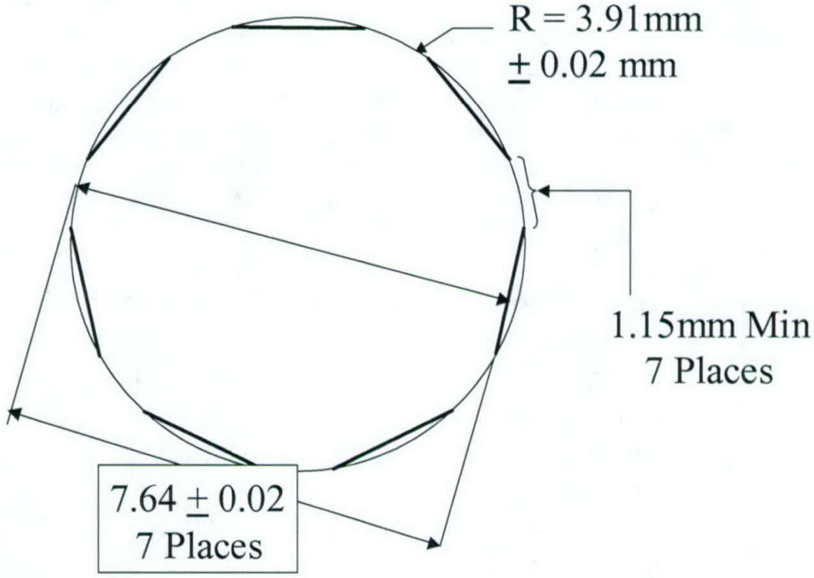

Figure 40
Revised heptagonal barrel configuration

CONCLUSIONS

1. The baseline heptagonal barrel will exhibit peak chamber pressures about 15 to 20% higher than the same cartridge loaded in a standard M240 barrel. This is due primarily to the increased resistance pressure early in the in bore travel of the projectile.

2. The increase in peak chamber pressure could be reduced by either increasing the free run of the projectile prior to the start of engraving or by reducing the forcing cone angle in the barrel.

3. A slight decrease in resistance force was observed for the 2.5 deg half angle forcing cone compared to the 1.2 deg half angle forcing cone found on the M240 barrel baseline. It is believed this difference is due to a reduction in the plastic deformation of the M80 projectile in the 1.2 deg barrel.

4. The addition of lubrication to the M80 projectile exterior increased the engraving force in the baseline M240 barrel with 1.2 deg half angle forcing cone, while it decreases the engraving forces in the 2.5 deg half angle forcing cone barrel. Likewise the push force standard deviation increased with lubrication in the 1.2 deg half angle forcing cone, and decreased in the 2.5 deg half angle forcing cone.

5. Projectile construction and elastic modulus appear to play significant roles in the resistance pressure of small caliber projectiles.

6. Unlubricated solid projectiles pushed in the heptagonal barrel resulted in push forces so high the push punch experienced catastrophic deformation.

RECOMMENDATIONS

1. The effect of forcing cone angle on resistance force should be more thoroughly explored for small caliber projectiles. Additional M240 and heptagonal barrel material is available for test samples, additional chamber reamers can be procured inexpensively from Clymer Tools at relatively short notice.

2. The effect of projectile construction on resistance pressure in the 2.5 deg half angle barrel and other forcing cones should be examined.

3. The "cross over" forcing cone angle between elastic and plastic projectile deformation should be determined for projectile designs using solid copper.

4. Longer barrel sections should be used for future testing to ensure accurate recording of the engraving pressure decay.

5. For future testing, the sample size should be increased (up to 50 or so) until a steady-state push force is achieved. Given the relative rapidity with which the data can be accumulated, this should not be a large cost driver.

6. Heptagonal barrel forcing cone design modifications should wait until further push tests with different forcing cone angles are completed on the current barrel configuration.

BIBLIOGRAPHY

1. Siewert, Jeff, "Final Report of the Rifling Profile Assessment Study," Contract DAAE30-00-M-0236, Arrow Tech Associates, Suite D-8, 1233 Shelburne Rd., S. Burlington, Vt. 05403, March 2002.

2. Private communications with Mr. Tim Janzen of Barnes Bullets, 19 May 2003.

3. www.clymertool.com website.

4. Wolf, J. Wolf and Cochran, G., "Rotating Band Rifling Interaction Study," Report 72APB552, General Electric, November 1972.

5. "PRODAS 2000 Users and Technical Manual", V3.0, Arrow Tech Associates, 1233 Shelburne Rd., Suite D-8, So. Burlington, VT 05403, Aug. 2002.

6. Private communication w/Larry Head of Federal Cartridge, 27 Feb 01, measured pressures of various diameter 30 caliber projectiles in 30-06 cartridge case.

7. Private communication with Mr. Bill Melton of Lake City Arsenal on M-80 projectile, 6 Sept 2000.

DISTRIBUTION LIST

USA ARDEC
ATTN: AMSRD-AAR-EMK (2)
AMSRD-AAR-GC
AMSRD-AAR-AEE-P (6)
Picatinny, NJ 07806-5000

Defense Technical Information Center (DTIC)
ATTN: Accessions Division
8725 John J. Kingman Road, Ste 0944
Fort Belvoir, VA 22060-6218

Commander
Soldier and Biological/Chemical Command
ATTN: AMSSB-CII, Library
Aberdeen Proving Ground, MD 21010-5423

Director
U.S. Army Research Laboratory
ATTN: AMSRL-CI-LP, Technical Library
Bldg. 4600
Aberdeen Proving Ground, MD 21005-5066

Chief
Benet Weapons Laboratory, AETC
U.S. Army Research, Development and Engineering Command
Armament Research, Development and Engineering Center
ATTN: AMSRD-AAR-AEW
Watervliet, NY 12189-5000

Director
U.S. Army TRADOC Analysis Center-WSMR
ATTN: ATRC-WSS-R
White Sands Missile Range, NM 88002

Chemical Propulsion Information Agency
ATTN: Accessions
10630 Little Patuxent Parkway, Suite 202
Columbia, MD 21044-3204

GIDEP Operations Center
P.O. Box 8000
Corona, CA 91718-8000